Discrete-Time Linear-Phase Nearly Orthogonal Wavelet Banks

Tapio Saramäki and Karen Egiazarian

Signal Processing Laboratory, Tampere University of Technology

P.O.Box 553, FIN-33101, Tampere, FINLAND

E-mails: ts@cs.tut.fi, karen@cs.tut.fi

ABSTRACT

A family of discrete-time linear-phase nearly orthogonal wavelet banks is introduced. These wavelet banks are intermediate cases between orthogonal wavelet banks having nonlinear-phase impulse responses and biorthogonal banks having linear-phase impulse responses. For these banks, the wavelet and scaling functions are made very regular and the wavelet function has several vanishing moments. Strightly speaking, the proposed filter banks are not real wavelet banks in the sense that there are negligible aliased terms and a very small reconstruction error for the unaliased component. Several examples are included showing the usefulness of the proposed banks in signal processing applications.

1   Introduction

Discrete-time finite impulse response (FIR) wavelet banks are usually constructed on the basis of perfect-reconstruction two-channel FIR filter banks having special properties [1]. This system consits of the analysis part and synthesis banks with the analysis and synthesis banks having lowpass-highpass filter pairs $H_0(z)$ and $H_1(z)$ and $F_0(z)$ and $F_1(z)$, respectively. In the case of lossless coding, the output signal $y(n)$ is a delayed version of the input signal $x(n)$, that is, $y(n) = x(n - N)$ (N is an odd integer) if

$$F_0(z) = H_1(-z), \; F_1(z) = -H_0(-z) \qquad (1a)$$

and

$$H_0(z)H_1(-z) - H_0(-z)H_1(z) = 2z^{-N}. \qquad (1b)$$

There are two conventional solutions satisfying these criteria, namely orthogonal and biorthogonal banks. In both cases, the sum of the orders of $H_0(z)$ and $H_1(z)$ is $2N$. For orthogonal banks, the orders of both $H_0(z)$ and $H_1(z)$ are N and

$$H_1(-z) = z^{-N}H_0(z^{-1}). \qquad (2)$$

In this case, $H_0(z)$ and $H_1(z)$ cannot possess exactly linear phase performances. In the biorthogonal case, $H_0(z)$ and $H_1(z)$ can be synthesized such that the impulse responses of $H_0(z)$ and $H_1(z)$ are symmetric and antisymmetric, respectively. These filters have to be designed to form a lowpass-highpass filter pair such that the sum of their orders is $2N$ and they satisfy the condition of Eq. (1b). The wavelet banks based on the use of these two-channel filter banks are usually made very regular with several vanishing moments by forcing $H_0(z)$ and $H_1(z)$ to have several zeros at $z = 1$ and $z = -1$, respectively.

The purpose of this paper is to design nearly orthogonal two-channel banks such that $H_0(z)$ and $H_1(z)$ have linear-phase responses. The price paid for the linear-phase performances is a small reconstruction error for the unaliased component and small aliasing errors for the resulting wavelet bank. These errors are tolerable in many applications where the perfect reconstruction is not needed because of the coding of the wavelet coefficients. Several examples are included illustrating the superiority of the proposed wavelet banks over other existing orthogonal banks in applications where the phase linearity is of importance.

2   Proposed Family of Wavelet Banks

This section introduces the proposed family of nearly orthonal linear-phase wavelet banks and shows how to optimize them.

2.1   Starting-Point Two-Channel Filter Bank

For the starting-point two-channel filter bank, it is assumed that

$$H_0(z) \equiv G(z) = \sqrt{2}\widehat{G}(z), \qquad (3a)$$

where

$$\widehat{G}(z) = E(z)\left(\frac{1 + z^{-1}}{2}\right)^M \qquad (3b)$$

with M being odd and

$$E(z) = \sum_{n=0}^{2L} e(n)z^{-n}, \quad e(2L - n) = e(n). \qquad (4)$$

The impulse response of $G(z)$ is thus symmetric and the order of $G(z)$ is $N = 2L + M$ that is an odd number. The corresponding length, $N + 1$, is an even number. Furthermore, it is assumed that

$$H_1(z) = H_0(-z) = G(-z) = \sqrt{2}\widehat{G}(-z), \qquad (5a)$$

$$F_0(z) = H_1(-z) = G(z) = \sqrt{2}\widehat{G}(z), \qquad (5b)$$

and

$$F_1(z) = -H_0(-z) = -G(-z) = -\sqrt{2}\widehat{G}(-z). \qquad (5c)$$

This two-channel filter bank is a special case of the banks proposed by Johnston [2] in the sense that all the zeros of $H_0(z)$ lying on the unit circle are forced to be located at $z = -1$.

In this case, the z-transforms of the input and output signals $x(n)$ and $y(n)$ are related through

$$Y(z) = T(z)X(z), \qquad (6a)$$

where

$$T(z) = [\widehat{G}(z)]^2 - [\widehat{G}(-z)]^2. \qquad (6b)$$

The corresponding frequency response is given by

$$T(e^{j\omega}) = e^{-j(M+2L)\omega} R(\omega), \qquad (7a)$$

where

$$R(\omega) = [S(\omega)\cos^M(\omega/2)]^2 + [S(\pi-\omega)\sin^M(\omega/2)]^2 \quad (7b)$$

with

$$S(\omega) = e(L) + 2\sum_{n=1}^{L} e(L-n)\cos n\omega. \qquad (7c)$$

2.2 Filter Optimization

Given M and L, the adjustable parameters $e(n)$ for $n = 0, 1, \cdots, L$ are desired to be optimized to be minimize

$$\epsilon = \max_{\omega \in [0,\,\pi]} |R(\omega) - 1| \qquad (8a)$$

subject to

$$e(L) + 2\sum_{n=1}^{L} e(L-n) = 1. \qquad (8b)$$

This means that the reconstruction error is minimized in the minimax sense subject to the condition that at the zero frequency this error is zero. For the optimization purposes, we have modified the second algorithm proposed by Dutta and Vidyasagar in [3].

2.3 Properties of the Resulting Wavelet Bank

For the K-stage wavelet bank, the input-output relation can be shown to be

$$Y(z) = \sum_{l=0}^{2^{K-1}-1} T_l^{(K)}(z) X(z e^{j2\pi l/2^{K-1}}), \qquad (9)$$

where for $K = 1$ and $K = 2$, respectively,

$$T_0^{(1)}(z) = [\widehat{G}(z)]^2 - [\widehat{G}(-z)]^2 \qquad (10)$$

and

$$T_0^{(2)}(z) = [\widehat{G}(z)]^2 T_0^{(1)}(z^2) - z^{-2N}[\widehat{G}(-z)]^2 \qquad (11a)$$

and

$$T_1^{(2)}(z) = \widehat{G}(z)\widehat{G}(-z)[T_0^{(1)}(z^2) - z^{-2N}]. \qquad (11b)$$

In the $K > 2$ case, the $T_l^{(K)}(z)$'s can be generated by using the following recursion formulas:

$$T_0^{(k)}(z) = [\widehat{G}(z)]^2 T_0^{(k-1)}(z^2) - z^{-2(2^{k-1}-1)N}[\widehat{G}(-z)]^2, \quad (12a)$$

$$T_{2^k-2}^{(k)}(z) = \widehat{G}(z)\widehat{G}(-z)[T_0^{(k-1)}(z^2) - z^{-2(2^{k-1}-1)N}], \quad (12b)$$

and for $l = 1, 2, \cdots, 2^{k-2} - 1$,

$$T_l^{(k)}(z) = \widehat{G}(z)\widehat{G}(z e^{j2\pi l/2^{k-1}}) T_l^{(k-1)}(z^2), \qquad (12c)$$

$$T_{l+2^{k-2}}^{(k)}(z) = \widehat{G}(z)\widehat{G}(z e^{j2\pi(l+2^{k-2})/2^{k-1}}) T_l^{(k-1)}(z^2). \quad (12d)$$

From the above equations, it is seen that in addition to the unaliased term $T_0^{(K)}(z) X(z)$, there are $2^{(K-1)} - 1$ aliased terms. Among then, the term $T_{2^K-2}^{(K)}(z) X(-z)$ has been observed to be the dominating one.

3 Optimized Filter Banks

The terms $T_0^{(K)}(z) X(z)$ and $T_{2^K-2}^{(K)}(z) X(-z)$ are of great importance when designing a K-level nearly orthogonal linear-phase wavelet bank. Both $T_0^{(K)}(z)$ and $T_{2^K-2}^{(K)}(z)$ are linear-phase FIR filter transfer functions of order $2(2^K-1)N$. The maximum reconstruction error for the unaliased component and the maximum aliased error are, respectively, given by

$$\epsilon^{(K)} = \max_{\omega \in [0,\,\pi]} |T_0(e^{j\omega}) - e^{-j(2^K-1)N\omega}| \qquad (13a)$$

and

$$\delta^{(K)} = \max_{\omega \in [0,\,\pi]} |T_{2^K-2}^{(K)}(e^{j\omega})|. \qquad (13b)$$

It has turned out that the following cases result in very small values for $\epsilon^{(K)}$ and $\delta^{(K)}$ also for a large value of K: $M = 3$, $L = 2$, $N = 2L + M = 7$; $M = 3$, $L = 3$, $N = 9$; $M = 5$, $L = 3$, $N = 11$; $M = 5$, $L = 4$, $N = 13$; $M = 7$, $L = 4$, $N = 15$; $M = 7$, $L = 5$, $N = 17$; $M = 9$, $L = 4$, $N = 17$; $M = 9$, $L = 5$, $N = 19$; $M = 11$, $L = 5$, $N = 21$; and $M = 11$, $L = 6$, $N = 23$.

Here, we consider in more details the $M = 7$ and $L = 5$ case. In this case, the impulse response coefficients of $H_0(z)$ are given by

$$h(0) = h(17) = 0.00077561, \ \ h(1) = h(16) = 0.00091432,$$

$$h(2) = h(15) = -0.00728739, \ \ h(3) = h(14) = -0.00224474,$$

$$h(4) = h(13) = 0.03634615, \ \ h(5) = h(12) = -0.01268065,$$

$$h(6) = h(11) = -0.12482346, \ \ h(7) = h(10) = 0.13432404,$$

$$h(8) = h(9) = 0.68178289.$$

In this case, $\epsilon^{(1)} = 0.0001786$, $\epsilon^{(2)} = 0.0003570$, $\epsilon^{(3)} = 0.0005157$, $\epsilon^{(4)} = 0.0005188$, $\epsilon^{(5)} = 0.0005189$, and $\delta^{(K)} = 0.00008149$ for $K = 2, 3, 4, 5$. Hence, these errors are practically negligible. The amplitude responses of $H_0(z)$ and $H_1(z)$ are shown in Fig. 1, whereas Figs. 2 and 3 show for several values of K the reconstruction error and the dominating aliased component.
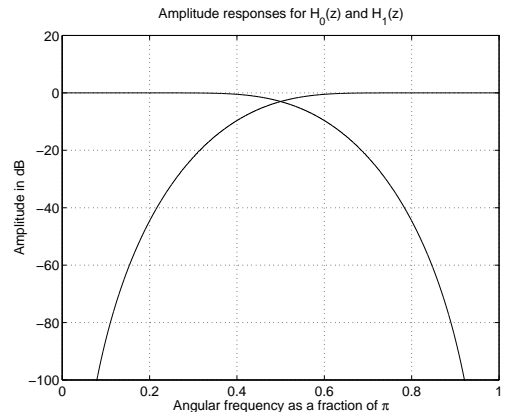

Figure 1: Amplitude responses for $H_0(z)$ and $H_1(z)$ in the $M = 7$ and $N + 1 = 18$ case.
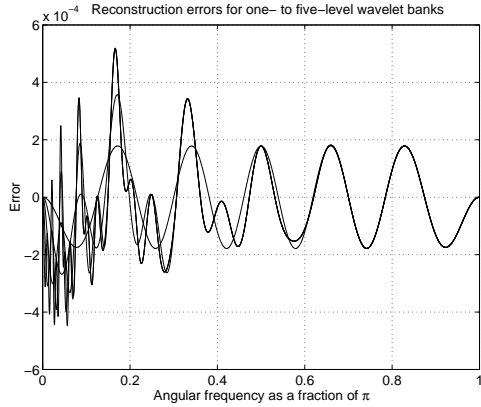
Figure 2: Reconstruction errors for one- to five-level wavelet banks in the $M = 7$ and $N + 1 = 18$ case.
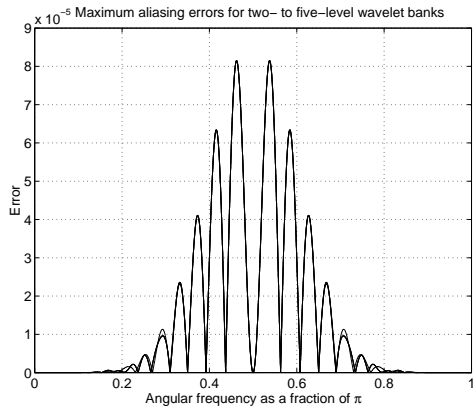

Figure 3: Maximum aliasing errors for two- to five-level wavelet banks in the $M = 7$ and $N + 1 = 18$ case.

4 Applications in De-Noising, Noisy Deconvolution, and Lossy Compression of Signals/Images

The noise reduction (de-noising) method by the nonlinear thresholding in the wavelet domain proposed by Donoho and Johnstone [4] consists of the following three steps: (1) transform the noisy data into an orthogonal domain, (2) Apply "hard" or "soft" thresholding to the resulting coefficients, which will yield a suppression of the coefficients of lower energy, and (3) Transform the result back to the original domain with the aid of the inverse transform. However, when using this scheme one may end up with some artifacts near singularities (pseudo-Gibbs phenomenon). One way to overcome this problem is to use undecimated (or stationary, shift-invariant) wavelet transforms [5] by applying the following simple strategy: wavelet de-noising is applied to all circular shifts of a signal, each of the particular result of de-noising is unshifted, and, finally, the average of all these results is generated [5]. Here we compare a fully translation-invariant de-noising using the stationary wavelet transforms based on "Coiflets" and "Symmlets", and the stationary version of pseudo-wavelet transform (NPR) proposed in this paper (all filters are of length 18). Figure 4 shows the de-noising results of a "Doppler" test signal (generated by Donoho's MATLAB

routine "MakeSignal" from his software package "WaveLab" [6]) of length 512. Five levels of decomposition have been used. Visually the performance of all these methods looks the same. Numerical performances have been estimated by the root mean square error (RMSE) and the mean absolute error (MAE):

(RMSE,MAE)("Noisy input")=(23.06, 0.82);
(RMSE,MAE)("Symmlet")=(9.39,0.27);
(RMSE,MAE)("Coiflet")=(9.91,0.28);
(RMSE,MAE)("NPR")=(8.85,0.26).

For the proposed pseudo-wavelet bank, $N + 1 = 18$, $M = 7$, $\epsilon^{(5)} = 0.000519$, and $\delta^{(5)} = 0.000081$.
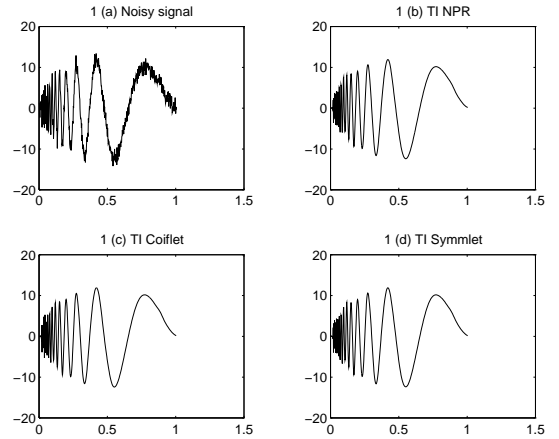

Figure 4: Noisy "Doppler" signal and translation invariant wavelet de-noising using "Symmlet", "Coiflet" and linear phase pseudo wavelet.

Another application is the noisy deconvolution using the proposed pseudo-wavelets. Since the deconvolution problem is ill-posed, the application of the inverse filter will give an object which is extremely noisy and has no real resemblance to the original object. The idea is to apply thresholding in the wavelet domain with thresholds specially chosen to adapt to the structure of the deconvolution problem [6].

We have used three test signals: "Bumps", "Doppler" and "Cusp" (all of these test signals as well as the application of the wavelets to this problem can be found in the software package "WaveLab" [6]). Our test signals were convolved with a recursive filter that blurs out the sharp structure and then noise was added.

We have compared the results of deconvolution by applying some orthogonal wavelet transforms as well as the proposed pseudo-wavelet transforms. All these reconstructions are nearly noise free and well preserve the structure of the objects.

We have made 400 experiments (with each of the objects). The averaged results showing corresponding RMSE and MAE are given in Table 1. We have examined 3 different wavelet transforms: Daubechies (D9), Coiflet (C3), Symmlet (S9), and two pseudo-wavelets $P18 - 7$ ($N + 1 = 18$, $M = 7$) and $P18 - 9$ ($N + 1 = 18$, $M = 9$). The test signals were of the length 2048, and the transforms made 6 levels of decomposition. For a fair comparison, all the filter banks were selected to be of the same length 18.

The third application of pseudo-wavelets is a lossy image compression. Here we have used the best basis selection algorithm [7] in order to obtain the best wavelet packet bases for

Table 1: Quantitative results for noisy signal deconvolution

Transforms	Signals					
	"Bumps"		"Doppler"		"Cusp"	
	RMSE	MAE $\times 10^{-2}$	RMSE	MAE $\times 10^{-3}$	RMSE	MAE $\times 10^{-3}$
Daubechies (D9)	7.156	3.419	1.509	7.999	1.379	8.892
Symmlet (S9)	6.618	3.830	1.409	6.365	1.179	5.348
Coiflet (C3)	6.623	3.581	1.528	7.326	1.216	6.354
Pseudo (P18-7)	6.275	3.136	1.323	6.246	1.095	5.404
Pseudo (P18-9)	6.262	3.152	1.305	6.220	1.125	6.216

both an orthogonal "Symmlet" (S9) and the pseudo-wavelet $P18-7$ for the test image "Lenna" (256×256). Then, this image has been compressed in these bases keeping the largest (in the absolute value) coefficients. In Fig. 5 the best 7% reconstructions for both cases are shown.

In addition to better numerical performances of the proposed scheme, pseudo-wavelet transforms can be implemented more efficiently.

5 Acknowledgement

References

[1] Vetterli, M. and Kovacevic, J. *Wavelets and Subband Coding*. Prentice Hall, 1995.

[2] Johnston, J. D. "A filter family designed for use in quadrature mirror filter banks," *IEEE International Conference on Acoustics, Speech and Signal Processing*, Denver, Colorado, April 1980, pp. 291-294.

[3] Dutta, S. R. K. and Vidyasagar, M. "New algorithms for constrained minimax optimization," *Mathematical Programming*, vol. 13, 1977, pp. 140-155.

[4] Donoho, D. "De-noising by soft thresholding," *IEEE Transactions on Information Theory*, vol. 41, 1995, pp. 613-627.

[5] Coifman, R. R. and Donoho, D. L. "Translation-Invariant de-noising," in *Wavelets and statistics*, Springer-Verlag, 1995, pp. 125-150.

[6] WaveLab web page (WaveLab .701) http://playfair.stanford.edu/ wavelab/.

[7] Wickerhauser, M. V. *Adapted Wavelet Analysis from Theory to Software*, IEEE Press, A.K.Peters, Wellesley, Massachusetts, 1994.
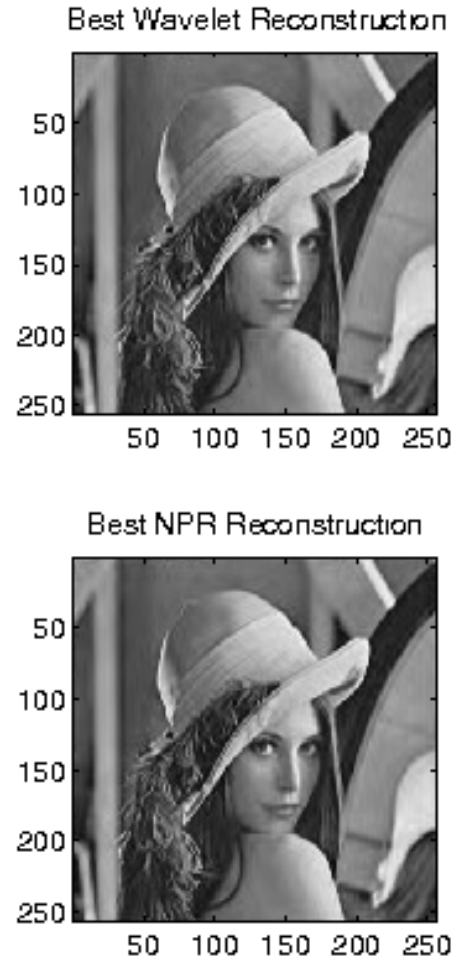

Figure 5: Best 7% reconstructions from compressed image "Lenna" using the wavelet packet (S9) and pseudo-wavelet packet (P18-7)